
**Interventricular Mechanical Asynchrony in Pulmonary Arterial Hypertension: Left-to-Right Delay in Peak Shortening Is Related to Right Ventricular Overload and Left Ventricular Underfilling**

J. Tim Marcus, C. Tji-Joong Gan, Jaco J.M. Zwanenburg, Anco Boonstra, Cor P. Allaart, Marco J.W. Götte, and Anton Vonk-Noordegraaf

*J. Am. Coll. Cardiol.* 2008;51;750-757
doi:10.1016/j.jacc.2007.10.041



Journal of the American College of Cardiology
© 2008 by the American College of Cardiology Foundation
Published by Elsevier Inc.

Vol. 51, No. 7, 2008
ISSN 0735-1097/08/$34.00
doi:10.1016/j.jacc.2007.10.041



# Interventricular Mechanical Asynchrony in Pulmonary Arterial Hypertension

## Left-to-Right Delay in Peak Shortening Is Related to Right Ventricular Overload and Left Ventricular Underfilling

J. Tim Marcus, PHD,* C. Tji-Joong Gan, MSC,† Jaco J. M. Zwanenburg, PHD,§ Anco Boonstra, MD, PHD,† Cor P. Allaart, MD, PHD,‡ Marco J. W. Götte, MD, PHD,‡ Anton Vonk-Noordegraaf, MD, PHD†

*Amsterdam and Utrecht, the Netherlands*

**Objectives** The purpose of this study was to explore in pulmonary arterial hypertension (PAH) whether the cause of interventricular asynchrony lies in onset of shortening or duration of shortening.

**Background** In PAH, leftward ventricular septal bowing (LVSB) is probably caused by a left-to-right (L-R) delay in myocardial shortening.

**Methods** In 21 PAH patients (mean pulmonary arterial pressure 55 ± 13 mm Hg and electrocardiogram–QRS width 100 ± 16 ms), magnetic resonance imaging myocardial tagging (14 ms temporal resolution) was applied. For the left ventricular (LV) free wall, septum, and right ventricular (RV) free wall, the onset time ($T_{onset}$) and peak time ($T_{peak}$) of circumferential shortening were calculated. The RV wall tension was estimated by the Laplace law.

**Results** The $T_{onset}$ was 51 ± 23 ms, 65 ± 4 ms, and 52 ± 22 ms for LV, septum, and RV, respectively. The $T_{peak}$ was 293 ± 58 ms, 267 ± 22 ms, and 387 ± 50 ms for LV, septum, and RV, respectively. Maximum LVSB was at 395 ± 45 ms, coinciding with septal overstretch and RV $T_{peak}$. The L-R delay in $T_{onset}$ was −1 ± 16 ms ($p = 0.84$), and the L-R delay in $T_{peak}$ was 94 ± 41 ms ($p < 0.001$). The L-R delay in $T_{peak}$ was not related to the QRS width but was associated with RV wall tension ($p < 0.05$). The L-R delay in $T_{peak}$ correlated with leftward septal curvature ($p < 0.05$) and correlated negatively with LV end-diastolic volume ($p < 0.05$) and stroke volume ($p < 0.05$).

**Conclusions** In PAH, the L-R delay in myocardial peak shortening is caused by lengthening of the duration of RV shortening. This L-R delay is related to LVSB, decreased LV filling, and decreased stroke volume. (J Am Coll Cardiol 2008; 51:750–7) © 2008 by the American College of Cardiology Foundation

In pulmonary arterial hypertension (PAH), leftward ventricular septal bowing (LVSB) is most prominent during early left ventricular (LV) diastole (1,2,3) and impairs LV filling (4,5,6,7). Leftward ventricular septal bowing has been assessed by cine magnetic resonance imaging (MRI) and echocardiography (1,8) and can be quantified by the radius of leftward curvature (9). By MRI and tissue Doppler imaging (6,10,11), a right ventricular (RV) delay in the time to peak strain was observed in PAH. Such a left-to-right delay induces a left-to-right transseptal pressure gradient that might be the mechanism causing LVSB (12). However, in these studies it was not yet clear whether this delay was caused by delayed RV onset or prolonged RV shortening.

See page 758

The cause of either delayed or prolonged RV shortening is unknown, and knowledge of this cause could have implications for treatment. A first potential mechanism is an electrical conduction delay: RV overload and concomitant remodeling might well lead to a (partial) right bundle branch block (RBBB), left-to-right electrical dyssynchrony, and subsequent mechanical dyssynchrony. This would become manifest as a delayed RV time to onset of shortening in comparison with the LV. An alternative mechanism

From the Departments of *Physics and Medical Technology, †Pulmonary Diseases, and ‡Cardiology, Institute for Cardiovascular Research, VU University Medical Center, Amsterdam, the Netherlands; and the §Image Sciences Institute, University Medical Center Utrecht, Utrecht, the Netherlands. C.T. Gan was financially supported by the Netherlands Organisation for Scientific Research (NWO), Mozaiek Grant, project number 017.001.154. Dr. Zwanenburg was financially supported by the Netherlands Heart Foundation, grant number NHF-2000B220.

Manuscript received August 8, 2006; revised manuscript received October 10, 2007, accepted October 22, 2007.

could be initiated directly by the mechanical pressure and volume overload, inducing increased RV wall tension and prolonged RV myocardial shortening. In this case, the time to onset of shortening would be similar for both ventricles, whereas the time to peak shortening of the RV wall would be delayed compared with the LV.

For the measurement of the left-to-right differences in the timing of shortening, MRI tagging and strain analysis provide a tool for accurate regional mapping of the onset and peak times in the myocardial wall (13). By this technique, any potential difference between RV and LV in onset times and peak times, to be denoted by the left-to-right (L-R) onset delay and the L-R peak delay, can be measured.

The aim of this study is to explore in PAH whether the cause of the L-R delay lies in the onset of shortening, in the duration of shortening, or in both. The relative roles of conduction delay and prolonged shortening due to overload might then be revealed. In addition, the functional impact of the L-R mechanical asynchrony is determined by assessing its association with LVSB, LV filling, and stroke volume.

## Methods

**Patients and control subjects.** Twenty-one patients with PAH, referred to the VU Medical Center for treatment, were recruited. The study was approved by the medical ethical committee of the VU Medical Center. Eleven healthy control subjects were included (age 38 ± 9 years, 6 women), with normal electrocardiogram (ECG) and QRS width of 80 ± 12 ms. In 2 control subjects, the pulmonary arterial pressure (PAP) was measured invasively, resulting in 24 ± 1 mm Hg, 8 ± 4 mm Hg, and 16 ± 2 mm Hg for systolic, diastolic, and mean values, respectively.

**Image acquisition.** A 1.5-T Siemens Sonata whole body MRI system, equipped with a 6-element phased-array coil, was used (Siemens Medical Solutions, Erlangen, Germany). The Siemens ECG gating system was used, with no known delay between the true QRS complex and the QRS complex used to trigger the sequence. The MRI myocardial tagging with high temporal resolution (14 ms) was applied with Complementary Spatial Modulation of Magnetization (7 mm tag distance) and steady state free precession imaging. Parameters: three phase-encoding lines/beat, repetition time 4.7 ms, echo time 2.3 ms, no view sharing, flip angle 20°, voxel size 1.2 × 3.8 × 6.0 $mm^3$. In all patients and control subjects this tagging cine was acquired in the mid-ventricular short-axis plane (13,14). In a subset of 9 patients (Patients #1 through #8 and #10) this tagging cine was also acquired in the basal and apical short-axis planes, to explore any effect of the longitudinal level on the timing of strain.

After the tagging acquisitions, the LV and RV were covered by a stack of short-axis cine MRI images, with steady state free precession imaging with a temporal resolution between 25 and 35 ms. In addition, cine images were acquired in the LV 3-chamber view showing the aortic and mitral valves and through the RV outflow tract showing the pulmonary valves. Finally, the flow was measured in the main pulmonary artery by MRI velocity quantification (temporal resolution 22 ms, velocity sensitivity 120 cm/s).

**Timing parameters derived from strain.** The tagged images were analyzed with the Harmonic Phase procedure (15). Circumferential shortening was calculated over time during the cardiac cycle. For the LV free wall, septum, and RV free wall, the onset time ($T_{onset}$) and peak time ($T_{peak}$) of circumferential shortening were calculated related to the ECG R-wave by automated routines (13). Overstretch is circumferential lengthening beyond end-diastolic value (or "positive strain"). Overstretch was observed in the septum and quantified by the peak lengthening and the time to peak lengthening.

**LV free wall, RV free wall, and septum definitions.** The LV free wall was subdivided in 5 equal segments. The 2 segments of the LV wall that were in direct continuity with the septum were not included as part of the LV free wall. The RV free wall was delineated in the same way. The complete septum was taken for the calculation of the septal strain, from the anterior until the posterior connections with the ventricular wall. For the LV free wall, RV free wall, and septum, the strains and strain timing parameters were derived. The difference between RV and LV in time to onset of shortening is denoted by the L-R delay in $T_{onset}$ and the difference in $T_{peak}$ by the L-R delay in $T_{peak}$.

**Timing parameters of the valves.** The time to aortic valve closure was derived from the 3-chamber cine. The time to pulmonary valve closure was derived from the RV outflow tract cine. In Patients #8 through #11 this pulmonary valve timing was derived from the most basal short-axis cine that showed the valves during the last part of systole.

**Global LV and RV parameters.** The stack of short-axis cine images was used for the calculation of the LV and RV end-diastolic volumes (EDVs) and the RV end-systolic volume (ESV). The RV stroke volume was measured from the flow map in the main pulmonary artery. The maximal leftward septal curvature was measured at the most basal short-axis cine slice that still showed the LV and RV myocardium through the cardiac cycle. The septal coordinates were marked at the anterior and posterior insertions

**Abbreviations and Acronyms**

- **BSA** = body surface area
- **ECG** = electrocardiogram
- **EDV** = end-diastolic volume
- **L-R delay** = left-to-right ventricular delay in circumferential shortening
- **LV** = left ventricle/ventricular
- **LVSB** = leftward ventricular septal bowing
- **MRI** = magnetic resonance imaging
- **PAH** = pulmonary arterial hypertension
- **PAP** = pulmonary arterial pressure
- **RBBB** = right bundle branch block
- **RV** = right ventricle/ventricular
- **$T_{onset}$** = time to onset of circumferential shortening
- **$T_{peak}$** = time to peak of circumferential shortening

**Table 1** Patient Characteristics

| Patient # | Gender, Age (yrs) | Diagnosis | HR (beats/min) | BP S/D (mm Hg) | PAP S/D/M (mm Hg) | QRS Width (ms) | RVEF (%) | NYHA Functional Class | Medication |
|---|---|---|---|---|---|---|---|---|---|
| 1 | F, 30 | IPAH | 78 | 100/50 | 101/35/62 | 96 | 53 | 3 | Epoprostenol |
| 2 | M, 56 | CTEPH | 67 | 110/80 | 71/28/47 | 138, RBBB | 10 | 3 | None |
| 3 | F, 45 | IPAH | 71 | 120/90 | 84/31/49 | 96 | 44 | 2 | Endothelin receptor antagonist |
| 4 | M, 56 | IPAH | 61 | 110/75 | 93/34/54 | 120 | 19 | 3 | Endothelin receptor antagonist |
| 5 | F, 52 | IPAH | 81 | 110/50 | 102/34/61 | 96 | 41 | 3 | Epoprostenol |
| 6 | M, 51 | CTEPH | 74 | n.a. | 83/33/51 | 100, inc. RBBB | 36 | 2 | None |
| 7 | F, 48 | IPAH | 86 | 120/70 | 97/32/57 | 120, inc. RBBB | 37 | 4 | Endothelin receptor antagonist |
| 8 | F, 34 | IPAH | 57 | 115/65 | 41/15/28 | 90 | 50 | 2 | Ca-antagonist |
| 9 | F, 23 | IPAH | 88 | 110/80 | 109/38/64 | 90 | 32 | 3 | Endothelin receptor antagonist |
| 10 | F, 41 | IPAH | 102 | 120/80 | 77/40/53 | 94, inc. RBBB | 27 | 3 | None |
| 11 | F, 38 | IPAH | 105 | 115/72 | 112/37/70 | 86 | 23 | 3 | Epoprostenol |
| 12 | F, 50 | CTEPH | 85 | 120/80 | 64/21/38 | 102 | 53 | 3 | Diltiazem; endothelin receptor antagonist |
| 13 | F, 26 | IPAH | 103 | n.a. | 87/38/60 | n.a. | 16 | 3 | Treprostenil; endothelin receptor antagonist; sildenafil |
| 14 | F, 27 | IPAH | 75 | 90/70 | 89/39/58 | 94 | 15 | 3 | Epoprostenol; endothelin receptor antagonist; sildenafil |
| 15 | M, 76 | IPAH | 80 | 120/80 | 88/29/52 | 78 | 38 | 3 | Epoprostenol |
| 16 | M, 16 | IPAH | 80 | 122/67 | 130/57/90 | 118 | 20 | 3 | Treprostenil; sildenafil; endothelin receptor antagonist |
| 17 | F, 56 | IPAH | 57 | 135/80 | 98/35/56 | 108 | 23 | 3 | Sildenafil; endothelin receptor antagonist |
| 18 | F, 36 | CTEPH | 92 | 100/70 | 92/33/58 | n.a. | 16 | 3 | Endothelin receptor antagonist; sildenafil |
| 19 | F, 58 | CTEPH | 70 | n.a. | 89/34/55 | 75 | 10 | 3 | Endothelin receptor antagonist |
| 20 | F, 41 | IPAH | 80 | 100/60 | 49/11/32 | 75 | 48 | 3 | Epoprostenol; sitaxentan sildenafil |
| 21 | F, 45 | IPAH | 98 | 105/65 | 79/34/50 | n.a. | 13 | 3 | Epoprostenol; sildenafil; endothelin receptor antagonist |

The "n.a." indicates that the value is not measured within 1 week of the magnetic resonance imaging investigation and catheterization.

BP = blood pressure; CTEPH = Chronic Thrombo-Embolic Pulmonary Hypertension; HR = heart rate; inc. = incomplete; IPAH = Idiopathic Pulmonary Arterial Hypertension; NYHA = New York Heart Association; PAP = pulmonary arterial pressure; RBBB = right bundle branch block; RVEF = right ventricular ejection fraction; S/D/M = systolic/diastolic/mean.

into the LV wall and at the middle of the septum. From these coordinates, the curvature was calculated (9).

**RV wall tension.** Our estimation of RV wall tension starts from the law of Laplace for a thin-walled sphere (16):

Wall tension = 0.5 × pressure × radius

The RV pressure during shortening is estimated by the systolic PAP. The RV-radius of curvature is difficult to measure directly because of the RV's irregular shape. Therefore, we estimate this radius from the RV ESV by assuming that this volume can be described by a sphere in PAH patients. Then the mean RV-radius is $0.620 \times (\text{RV-ESV})^{1/3}$. Finally, to be able to compare different patients with different body sizes, the RV radius is normalized to BSA (body surface area). The estimation of RV wall tension then becomes:

RV wall tension = 0.5 × PAPsystolic × RVradius/BSA

**Statistics.** Values are expressed as mean ± SD. First, the timing parameters were tested for a normal distribution by the Shapiro-Wilks test. Then, comparisons between LV and RV timing parameters were performed with the paired-samples *t* test (2-tailed). By the same test, the $T_{peak}$ in the RV wall was compared with the times of LVSB, septal overstretch, and pulmonary valve closure. Comparisons between patients and control subjects were performed by independent samples *t* testing (2-tailed). The relations between the L-R delay in $T_{peak}$

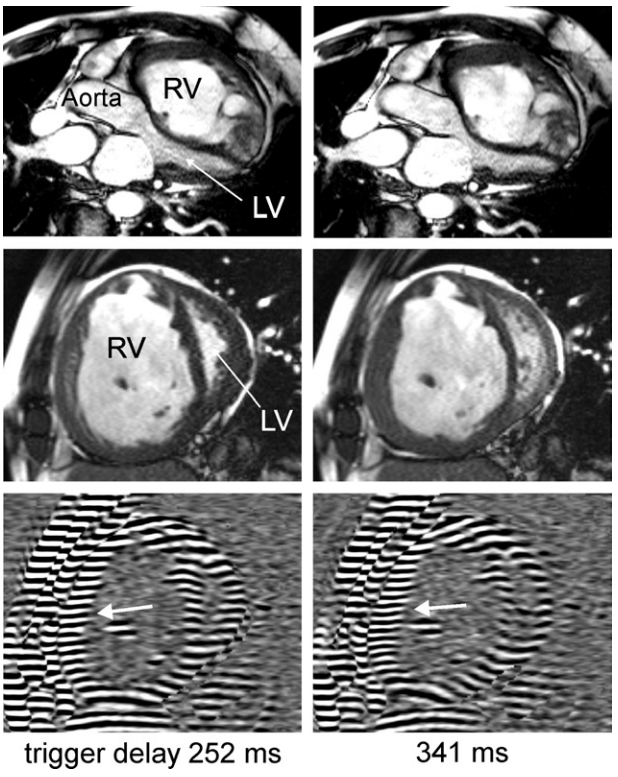


**Figure 1** MRI Cine and Tagged Images

Three-chamber images **(top panels)**, short-axis images **(middle panels)**, and short-axis tagged images **(bottom panels)**, at the time of aortic valve closure at trigger delay of 252 ms **(left)** and the time of peak right ventricular (RV) shortening at 341 ms **(right)**. The 3-chamber images show that maximal leftward septal bowing occurs at 341 ms, well after aortic valve closure. In the tagged image at 341 ms, the distance of the tagging lines in the RV free wall show further shortening **(thick white arrows)**, whereas the tagging lines in the left ventricular (LV) free wall show relaxation. MRI = magnetic resonance imaging.

versus ECG-QRS width, PAP, and RV wall tension were tested by linear regression. The relations between septal curvature, stroke volume (SV), and LV EDV versus the L-R delay in $T_{peak}$ were also tested by linear regression. In these regression tests, the L-R delay in $T_{peak}$ was normalized for the R to R interval (RR) of the individual patient.

The interobserver variation was determined for the $T_{peak}$ of the RV by Bland-Altman analysis, for a subset of 10 patients.

## Results

**Patient characteristics.** Sixteen patients were diagnosed as having idiopathic PAH, whereas 5 had chronic thromboembolic PAH. The systolic, diastolic, and mean PAPs were 87 ± 20 mm Hg, 33 ± 9 mm Hg, and 55 ± 13 mm Hg, respectively, as measured via right heart catheterization with a Swan-Ganz catheter. The medication at the time of the MRI is listed in Table 1. The ECG-QRS width was 100 ± 16 ms. On the basis of the ECG morphology, 3 patients had

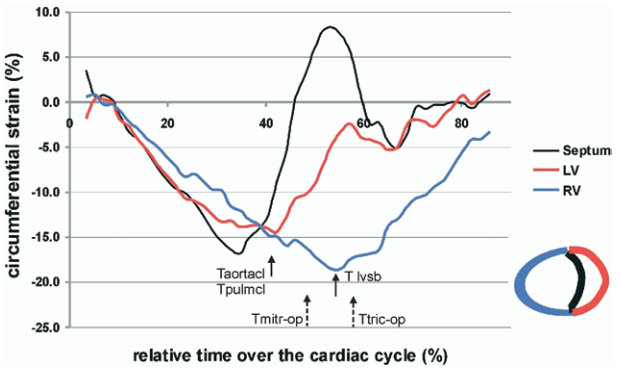


**Figure 2** Circumferential Strain Over Time, PAH Patient

Circumferential strain curves over time after the electrocardiographic R-wave for the left ventricular (LV) and right ventricular (RV) free walls and the septum for 1 patient at basal level. The LV, RV, and septum start simultaneously with shortening (negative strain), but the RV reaches its peak later than the LV, by 12% of the cardiac cycle time. The closure times of aortic and pulmonary valves ($T_{aortacl}$ and $T_{pulmcl}$) are coincident with the peak of LV shortening. The time of maximal leftward septal bowing ($T_{lvsb}$) is coincident with septal stretching (positive strain) and with the peak of RV shortening. The opening times of mitral and tricuspid valves ($T_{mitr\text{-}op}$ and $T_{tric\text{-}op}$) indicate the onset times of LV and RV filling. PAH = pulmonary arterial hypertension.

an incomplete RBBB, and 1 patient had a complete RBBB. The RV SV was 53 ± 19 ml, RV EDV 202 ± 69 ml, RV free wall mass 91 ± 56 g, LV mass 114 ± 27 g, LV EDV 105 ± 28 ml, LVEF 51 ± 12%, BSA 1.85 ± 0.26 $m^2$, and leftward septal curvature was 0.14 ± 0.05 $cm^{-1}$. The LV EDV in the patients was smaller than in the control subjects (105 ± 28 ml vs. 158 ± 36 ml, p = 0.001).

**Images and strains.** Figure 1 shows 3-chamber cine images, short-axis cine images, and short-axis tagged images at the time of aortic valve closure and at the time of maximal LVSB. In the patients, peak circumferential shortening of the LV and RV free walls was −14 ± 4% and −14 ± 3%, respectively (p = 0.88). Peak LV circumferential shortening in the patients

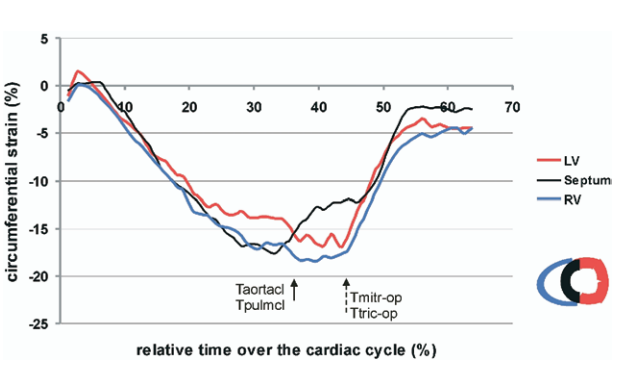


**Figure 3** Circumferential Strain Over Time, Healthy Subject

Similar to Figure 2 but for a healthy control subject. The RV reaches its peak slightly earlier than the LV, but LV and RV start relaxation simultaneously, and the septum does not overstretch. Abbreviations as in Figure 2.

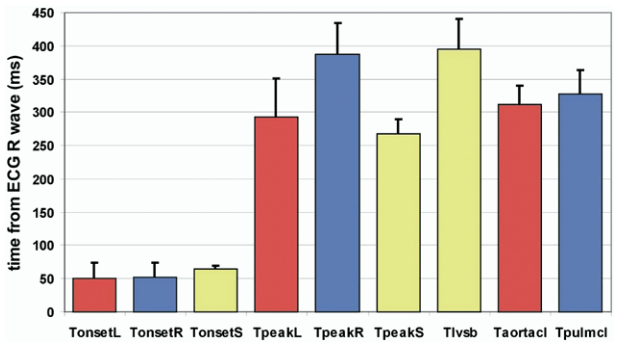


**Figure 4** Timing Parameters

Timing parameters presented by mean values and SDs (error bars), for the 21 pulmonary arterial hypertension patients. ECG = electrocardiogram; L = left ventricle; R = right ventricle; S = septum; $T_{aortacl}$ = closure time of aortic valve; $T_{ivsb}$ = time of maximal leftward septal bowing; $T_{onset}$ = onset time of circumferential shortening; $T_{peak}$ = peak time of circumferential shortening; $T_{pulmcl}$ = closure time of pulmonary valve.

was smaller than in the control subjects (−14 ± 4% vs. −20 ± 2%, $p < 0.001$). For the septum, peak shortening was −11 ± 3%, and the maximal overstretch was 6 ± 2%. Figure 2 shows the circumferential shortening curves during the cardiac cycle for the LV and RV free walls and the septum. The LV and RV start simultaneously, but the RV reaches its peak later than the LV. The septum shows overstretch (positive shortening) at the same time that the RV reaches its peak shortening.

In Figure 3, the same plot is given for a healthy control subject. In this control, the RV peak is not later than the LV peak, and the septum does not overstretch.

**Timing parameters.** The results of the timing parameters are given in Figure 4 and Table 2. In Table 2 the data from the control subjects are included. The differences between the timing parameters are presented in Table 3. As shown in Table 3, there is no L-R delay in $T_{onset}$, in contrast to the large L-R delay in $T_{peak}$ of 94 ± 41 ms ($p < 0.001$). In addition, $T_{peak}RV$ is $>T_{pulmcl}$ by 59 ± 40 ms, meaning that the RV free wall shows considerable post-systolic shortening, which does not contribute to ejection. The time of septal overstretch ($T_{stretch}$) is not different from the $T_{peak}RV$ ($p = 0.93$). Also the time of LVSB and the $T_{peak}RV$ are not different ($p = 0.60$). In the patients with an RBBB, the L-R delay in $T_{peak}$ was not different from the L-R delay in patients without an RBBB. In the control subjects, no L-R delay in timing was observed.

**Regression analysis of timing parameters.** By regression analysis, there was no relationship between the L-R delay in $T_{peak}$ and the L-R delay in $T_{onset}$ ($p = 0.91$). Also, the L-R delay in $T_{peak}$ was not associated with the ECG-QRS width ($p = 0.65$) or PAP-systolic (Table 4). As shown in Table 4

**Table 3** Paired-Samples *t* Tests (2-tailed) Between Timing Parameters of the Patients

| Sample 1 | Sample 2 | Sample 1 − Sample 2 = Difference (ms) | p Value |
|---|---|---|---|
| $T_{onset}LV$ | $T_{onset}RV$ | −1 ± 16 | 0.70 |
| $T_{onset}LV$ | $T_{onset}S$ | −4 ± 16 | 0.50 |
| $T_{peak}LV$ | $T_{peak}RV$ | −94 ± 41 | <0.001 |
| $T_{peak}LV$ | $T_{peak}S$ | 38 ± 27 | 0.005 |
| $T_{Ivsb}$ | $T_{peak}RV$ | 8 ± 34 | 0.31 |
| $T_{stretch}S$ | $T_{peak}RV$ | −1 ± 28 | 0.93 |
| $T_{pulmcl}$ | $T_{peak}RV$ | −59 ± 40 | <0.001 |
| $T_{aortacl}$ | $T_{peak}LV$ | 14 ± 46 | 0.23 |
| $T_{aortacl}$ | $T_{pulmcl}$ | −17 ± 23 | 0.008 |

In the healthy control subjects, none of the above *t* tests resulted in a significant difference. Abbreviations as in Table 2.

**Table 2** Results of Timing Parameters in 21 Patients and 11 Healthy Control Subjects

| Timing Parameter | Abbreviation | Patients Mean ± SD (ms) | Control Subjects Mean ± SD (ms) | Difference | p Value |
|---|---|---|---|---|---|
| Time between 2 ECG R waves | RR | 770 ± 142 | 989 ± 129 | −219 ± 192 | <0.001 |
| Time to onset of shortening of LV free wall | $T_{onset}LV$ | 51 ± 23 | 29 ± 25 | 22 ± 34 | 0.94 |
| Time to onset of shortening of RV free wall | $T_{onset}RV$ | 52 ± 22 | 44 ± 32 | 8 ± 39 | 0.31 |
| Time to onset of shortening of septum | $T_{onset}S$ | 65 ± 4 | 54 ± 23 | 11 ± 23 | 0.62 |
| Time to peak of shortening of LV free wall | $T_{peak}LV$ | 293 ± 58 | 386 ± 68 | −93 ± 89 | <0.001 |
| Time to peak of shortening of RV free wall | $T_{peak}RV$ | 387 ± 50 | 350 ± 55 | 37 ± 74 | 0.15 |
| Time to peak shortening of septum | $T_{peak}S$ | 267 ± 22 | 339 ± 37 | −72 ± 43 | 0.24 |
| Time to overstretch of septum | $T_{stretch}S$ | 410 ± 16 | Not observed | | |
| Time to leftward ventricular septal bowing | $T_{Ivsb}$ | 395 ± 45 | Not observed | | |
| Time to pulmonary valve closure | $T_{pulmcl}$ | 328 ± 36 | 375 ± 36 | −47 ± 51 | <0.001 |
| Time to aortic valve closure | $T_{aortacl}$ | 311 ± 29 | 354 ± 16 | −43 ± 33 | <0.001 |

Comparisons were performed with independent-samples *t* testing (2-tailed).
ECG = electrocardiographic; LV = left ventricular; RV = right ventricular.

**Table 4** Results of Linear Regression Analysis

| Dependent Variable | Independent Variable | p Value | r | Slope | Intercept |
|---|---|---|---|---|---|
| $(T_{onset}RV - T_{onset}LV)/RR$ | QRS width (ms) | 0.99 | 0.1 | NS | NS |
| $(T_{peak}RV - T_{peak}LV)/RR$ | QRS width (ms) | 0.65 | 0.1 | NS | NS |
| $(T_{peak}RV - T_{peak}LV)/RR$ | PAP-systolic (mm Hg) | 0.11 | 0.36 | NS | NS |
| $(T_{peak}RV - T_{peak}LV)/RR$ | RV wall tension (mm Hg·cm·m$^{-2}$) | 0.01 | 0.55 | 0.0013 | 0.019 |
| Leftward septal curvature (cm$^{-1}$) | $(T_{peak}RV - T_{peak}LV)/RR$ | 0.03 | 0.64 | 0.73 | 0.05 |
| SV (ml/m$^2$) | $(T_{peak}RV - T_{peak}LV)/RR$ | 0.023 | 0.49 | −72.4 | 38.1 |
| LV-EDV (ml) | $(T_{peak}RV - T_{peak}LV)/RR$ | 0.02 | 0.50 | −213 | 132.4 |

RR is the ECG-derived time interval between 2 heartbeats. The large p values and low r values for the relations versus QRS width mean that the QRS width is not related to the left-to-right (L-R) asynchrony in mechanical timing.

EDV = end-diastolic volume; PAP = pulmonary arterial pressure; SV = stroke volume; other abbreviations as in Table 2.

and Figure 5, there was an association between the L-R peak delay and the RV wall tension ($p = 0.01$, $r = 0.55$). The L-R delay in $T_{peak}$ was related to leftward septal curvature ($p < 0.05$) and was negatively related to LV EDV ($p = 0.02$, $r = 0.50$) and RV stroke volume ($p = 0.023$, $r = 0.49$), as shown in Table 4.

**Regional analysis.** For the subset of 9 patients with base, mid, and apical coverage, the L-R difference in $T_{peak}$ was 85 ± 35 ms, 110 ± 51 ms, and 48 ± 57 ms at basal, mid, and apical levels, respectively. The effect of the level was not significant. Also, the $T_{peak}$ was measured in the RV anterior, RV lateral, and RV inferior subregions; no effect of these subregions was found.

**Reader agreement.** The interobserver variation in the $T_{peak}$ of the RV was given by a correlation coefficient of 0.88 with $p < 0.001$ and a bias of −5 ms with 95% confidence limits of agreement of −47 and +37 ms, respectively.

## Discussion

The results showed that in PAH there is a 94-ms L-R delay in $T_{peak}$ of shortening, which is caused by lengthening of the duration of RV shortening rather than a delay in the onset of RV shortening.

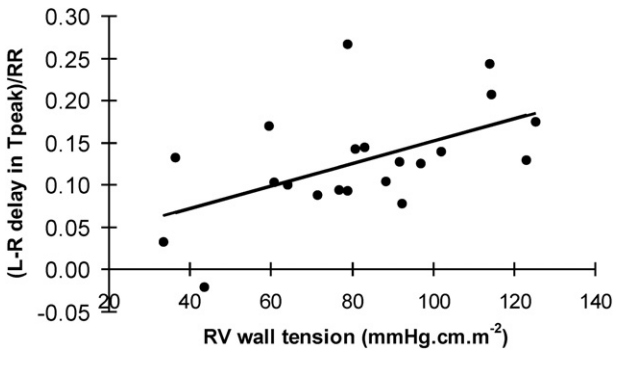


**Figure 5** L-R Delay Versus RV Wall Tension

Linear regression between the left-to-right (L-R) delay in time to peak of circumferential shortening ($T_{peak}$) normalized for the R to R interval (RR) as dependent variable and the right ventricular (RV) wall tension, $p = 0.01$, $r = 0.54$.

**Cause of L-R asynchrony in $T_{peak}$.** Because the L-R peak delay was not related to an L-R onset delay or the QRS width, it is unlikely that electrical conduction delay would be the only dominant factor responsible for the L-R peak delay. Instead, the mechanism of the prolonged RV systole in PAH is probably the increased RV wall tension as shown by the correlation between L-R peak delay and RV wall tension (Fig. 5). This mechanism is supported by measurements in rat cardiac trabeculae, which provided evidence that an increased load of myocytes leads to a slower and prolonged shortening velocity (17).

**LVSB.** The mechanism of LVSB is now better documented: maximal LVSB coincides with peak RV shortening and overstretch of the septal wall. Thus it is unlikely that there is compression of the septum, as suggested earlier (5). The overstretch indicates that LVSB is a result of higher

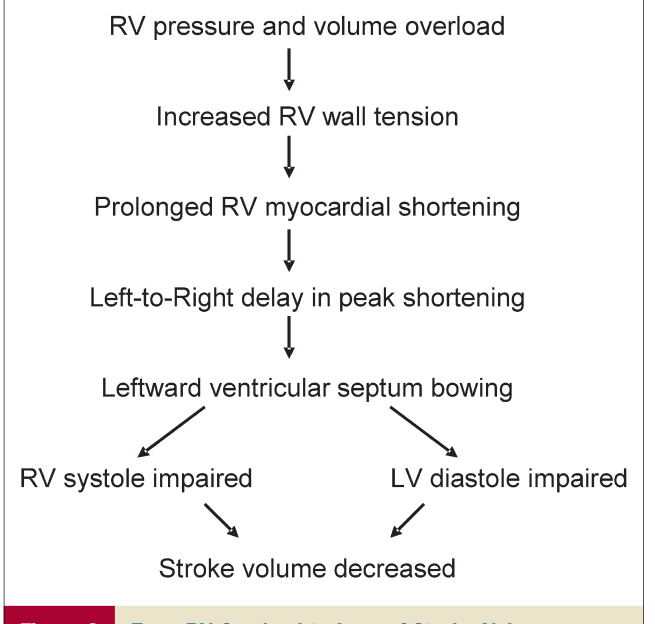


**Figure 6** From RV Overload to Loss of Stroke Volume

Flowchart of the proposed mechanism by which RV overload relates to a left-to-right delay in peak shortening, which relates to the loss of stroke volume in PAH. Only correlations were studied, so the cause-effect relationships in this flowchart are only a tentative postulated model. Abbreviations as in Figure 2.

pressure in the RV than in the LV, owing to the ongoing shortening in the RV free wall, whereas the LV free wall is already in its relaxation phase.

**Impaired RV systole.** The observed RV SV (53 ± 19 ml) is lower than normal reference values of 88 ± 19 ml (18) and showed a negative correlation with the L-R peak delay. This effect of the L-R peak delay can be explained: owing to the mechanical asynchrony between the RV free wall and the septum, the RV contraction is very inefficient in its late phase. As shown in the results, the $T_{peak}$ of the RV free wall is 120 ms after the $T_{peak}$ of the septum, and when finally the RV free wall reaches its peak shortening, the septum is shifted to the left. The observation that the $T_{peak}$RV is 59 ms later than the closure of the pulmonary valves (post-systolic shortening) further illustrates the inefficiency of this last part of RV myocardial shortening. The effective systole of the RV is estimated to begin at the onset of RV shortening (mean 52 ms) and to run until pulmonary valve closure (mean 328 ms), thereby taking 276 ms. With 59 ms post-systolic shortening, total RV shortening time is 335 ms, and thus (59/335) × 100% = 18% of total RV shortening time is wasted, and energy is dissipated in the nonfunctional LVSB. Thus the observed L-R asynchrony in PAH can be considered as an independent factor that has a negative effect on RV stroke volume. This is in line with earlier Doppler-echo observations showing that RV dyssynchrony is related to RV dysfunction in PAH (10,11,19) and also in line with the architectural disadvantage of a leftward bowed septum (20).

In principle the loss of RV forward stroke volume might also be caused by tricuspid regurgitation. However we found no significant difference between the RV SV derived from (RV EDV − RV ESV) and the RV SV derived from forward flow. This indicates that the volumetric contribution of tricuspid regurgitation to the loss of forward flow was minor.

**Impaired LV diastole.** As mentioned in the results, the L-R delay in $T_{peak}$ predicted leftward septal curvature and thereby had a negative effect on LV EDV. The negative relation between LVSB and LV filling was shown earlier in larger patient groups (7,12). This is confirmed in the present study, where the septum bowed maximally to the left at 395 ms, whereas the aortic valves had already been closed at 311 ms. Our observed negative association between L-R delay in $T_{peak}$ and LV EDV supports the concept that the L-R asynchrony plays a key role in the LV filling impairment. The impaired LV filling and the ineffective RV systolic function both contribute to the loss of stroke volume, as displayed in the flowchart in Figure 6.

The measured values of LV EDV were shown to be smaller than the healthy control values. Also the observed LV free wall peak shortening was smaller than in the healthy control subjects. This is well explained by the Frank-Starling effect: the LV myocardial muscle fibers are not stretched to their optimal length and thus are not able to perform their optimal shortening. This underfilled LV further contributes to the leftward septal bowing and inefficient RV systole. In addition, Gurudevan et al. (21) evaluated several different indicators of LV filling and showed that the LV underfilling is in large part responsible for the impaired LV relaxation pattern.

**Practical implications.** In clinical practice, understanding the meaning of LVSB is relevant, because it is much easier to measure than the strain-derived properties of LV, RV, and septal wall. The LVSB can directly be measured and timed from MRI cine imaging (9) or from echocardiography. This easily obtained timing of maximal LVSB coincides with the RV time to peak shortening. The time to LV peak circumferential shortening can be estimated by the time of aortic valve closure. Thus the L-R delay in peak shortening can be estimated from the time interval between aortic valve closure and LVSB. This provides an easy measure to follow individual PAH patients during treatment, also when MRI is not available.

Another potential implication can be derived from the key role that the L-R delay in peak shortening plays in the loss of LV and RV performance. Although conduction delay is not the cause of the L-R mechanical delay, the mechanical synchrony between the LV and RV might be improved by earlier electrical activation of the RV free wall with pacing. This early activation will shift the RV contraction period to an earlier time in the cardiac cycle and possibly also shorten it. Both effects might reduce RV post-systolic shortening, thereby improving both the RV efficiency and LV filling. However, this has not been proven. Whether this might be an effective approach to improve cardiac function in PAH must be tested first in animals, before it might be considered in patients.

**Study limitations.** The role of electrical conduction delay was indirectly estimated from the ECG-QRS width and the onset times of shortening. The true role of conduction delay still needs more exploration.

The RV load was estimated by the wall tension. The assumption that the RV in PAH can be described by a sphere needs confirmation. The estimation might be improved by taking the wall thickness into account to calculate wall stress. However, the RV wall thickness is difficult to define, owing to its trabeculated endocardial border.

## Conclusions

In PAH, no L-R delay was observed in the onset times of shortening, whereas a large L-R delay was observed in the times to peak shortening. Thus the L-R delay in myocardial peak shortening is caused by lengthening of the duration of RV shortening. An increased RV wall tension rather than electrical conduction delay is related to this interventricular mechanical asynchrony. Because wall tension is the product of pressure and radius, it means in practice that those PAH patients with an increased RV pressure combined with an enlarged RV volume will have increased RV wall tension

and thereby more L-R mechanical asynchrony in $T_{peak}$. This asynchrony is associated with leftward septal bowing, LV underfilling, and decrease in RV stroke volume.

**Reprint requests and correspondence:** Dr. J. Tim Marcus, Department of Physics and Medical Technology, VU University Medical Center, P.O. Box 7057, 1007 MB Amsterdam, the Netherlands. E-mail: jt.marcus@vumc.nl.

## REFERENCES

1. Dong SJ, Smith ER, Tyberg JV. Changes in the radius of curvature of the ventricular septum at end diastole during pulmonary arterial and aortic constrictions in the dog. Circulation 1992;86:1280–90.
2. Beyar R, Dong SJ, Smith ER, Belenkie I, Tyberg JV. Ventricular interaction and septal deformation: a model compared with experimental data. Am J Physiol 1993;265:H2044–56.
3. Moses DA, Axel L. Quantification of the curvature and shape of the interventricular septum. Magn Res Med 2004 Jul;52:154–63.
4. Marcus JT, Vonk Noordegraaf A, Roeleveld RJ, et al. Impaired left ventricular filling due to right ventricular pressure overload in primary pulmonary hypertension: noninvasive monitoring using MRI. Chest 2001;119:1761–5.
5. Nelson GS, Sayed-Ahmed EY, Kroeker CAG, et al. Compression of interventricular septum during right ventricular pressure loading. Am J Physiol Heart Circ Physiol 2001;280:H2639–48.
6. Vonk Noordegraaf A, Marcus JT, Gan CT, Boonstra A, Postmus PE. Interventricular mechanical asynchrony due to right ventricular pressure overload in pulmonary hypertension plays an important role in impaired left ventricular filling (abstr). Chest 2005;128 Suppl:628S–30S.
7. Gan CT, Lankhaar JW, Marcus JT, et al. Impaired left ventricular filling due to right-to-left ventricular interaction in patients with pulmonary arterial hypertension. Am J Physiol Heart Circ Physiol 2006;290:H1528–33.
8. Ricciardi MJ, Bossone E, Bach DS, Armstrong WF, Rubenfire M. Echocardiographic predictors of an adverse response to a nifedipine trial in primary pulmonary hypertension: diminished left ventricular size and leftward ventricular septal bowing. Chest 1999;116:1218–23.
9. Roeleveld RJ, Marcus JT, Faes TJ, et al. Interventricular septal configuration at MR imaging and pulmonary arterial pressure in pulmonary hypertension. Radiology 2005;234:710–7.
10. Lopez Candales A, Dohi K, Bazaz R, Edelman K. Relation of right ventricular free wall mechanical delay to right ventricular dysfunction as determined by tissue Doppler imaging. Am J Cardiol 2005;96:602–6.
11. Lopez Candales A, Dohi K, Rajagopalan N, et al., Right ventricular dyssynchrony in patients with pulmonary hypertension is associated with disease severity and functional class. Cardiovasc Ultrasound 2005;3:23.
12. Stojnic BB, Brecker SJ, Xiao HB, Helmy SM, Mbaisourroum M, Gibson DG. Left ventricular filling characteristics in pulmonary hypertension: a new mode of ventricular interaction. Br Heart J 1992;68:16–20.
13. Zwanenburg JJ, Gotte MJ, Kuijer JP, et al. Timing of cardiac contraction in humans mapped by high-temporal-resolution MRI tagging: early onset and late peak of shortening in lateral wall. Am J Physiol Heart Circ Physiol 2004;286:H1872–80.
14. Zwanenburg JJM, Kuijer JPA, Marcus JT, Heethaar RM. Steady-state free precession with myocardial tagging: CSPAMM in a single breathhold. Magn Reson Med 2003;49:722–30.
15. Osman NF, Kerwin WS, McVeigh ER, Prince JL. Cardiac motion tracking using CINE harmonic phase (HARP) magnetic resonance imaging. Magn Reson Med 1999;42:1048–60.
16. Norton JM. Toward consistent definitions for preload and afterload. Adv Physiol Educ 2001;25:53–61.
17. Van Heuningen R, Rijnsburger WH, Ter Keurs HE. Sarcomere length control in striated muscle. Am J Physiol Heart Circ Physiol 1982;242:H411–20.
18. Alfakih K, Plein S, Thiele H, Jones T, Ridgway JP, Sivananthan MU. Normal human left and right ventricular dimensions for MRI as assessed by turbo gradient echo and steady-state free precession imaging sequences. J Magn Reson Imaging 2003;17:323–9.
19. Rajagopalan N, Dohi K, Simon MA, et al., Right ventricular dyssynchrony in heart failure: a tissue Doppler imaging study. J Card Fail 2006;12:263–7.
20. Saleh S, Liakopoulos OJ, Buckberg GD. The septal motor of biventricular function. Eur J Cardiothorac Surg 2006;29 Suppl 1:S126–38.
21. Gurudevan SV, Malouf PJ, Auger WR, et al. Abnormal left ventricular diastolic filling in chronic thromboembolic pulmonary hypertension. True diastolic dysfunction or left ventricular underfilling? J Am Coll Cardiol 2007;49:1334–9.

# Interventricular Mechanical Asynchrony in Pulmonary Arterial Hypertension: Left-to-Right Delay in Peak Shortening Is Related to Right Ventricular Overload and Left Ventricular Underfilling

J. Tim Marcus, C. Tji-Joong Gan, Jaco J.M. Zwanenburg, Anco Boonstra, Cor P. Allaart, Marco J.W. Götte, and Anton Vonk-Noordegraaf

*J. Am. Coll. Cardiol.* 2008;51;750-757
doi:10.1016/j.jacc.2007.10.041